Structural and immunodiagnostic characterization of synthetic Antigen B subunits from *Echinococcus granulosus* and their evaluation as target antigens for cyst viability assessment

Daniela Pagnozzi[1*], Francesca Tamarozzi[2,3╪], Anna Maria Roggio[1], Vittorio Tedde[1], Maria Filippa Addis[1╡], Salvatore Pisanu[1], Gabriella Masu[4], Cinzia Santucciu[4], Ambra Vola[3,5], Adriano Casulli[6,7], Giovanna Masala[4], Enrico Brunetti[2,3,5], Sergio Uzzau[1,8]

1 Porto Conte Ricerche, Science and Technology Park of Sardinia, Tramariglio, Alghero (Sassari), Italy
2 Department of Clinical, Surgical, Diagnostic and Pediatric Sciences, University of Pavia, Italy
3 WHO Collaborating Centre for the Clinical Management of Cystic Echinococcosis, Pavia, Italy
4 National Reference Laboratory of Cystic Echinococcosis, Istituto zooprofilattico sperimentale della Sardegna "G. Pegreffi", Sassari, Italy.
5 Division of Infectious and Tropical Diseases, IRCCS San Matteo Hospital Foundation, Pavia, Italy
6 WHO Collaborating Centre for the Epidemiology, Detection and Control of Cystic and Alveolar Echinococcosis, Department of Infectious Diseases, Istituto Superiore di Sanità, Rome, Italy
7 European Union Reference Laboratory for Parasites (EURLP), Department of Infectious Diseases, Istituto Superiore di Sanità, Rome, Italy
8 Department of Biomedical Sciences, University of Sassari, Sassari, Italy
╪ C*urrent affiliation: Centre for Tropical Diseases, Ospedale Sacro Cuore Don Calabria, Negrar, Verona, Italy*
╡ C*urrent affiliation: Department of Veterinary Medicine, University of Milan, Italy*

*Correspondence: Daniela Pagnozzi, PhD, Porto Conte Ricerche Srl, S.P. 55 Porto Conte - Capo Caccia, km 8,400 Loc. Tramariglio - 07041 Alghero (SS) - Italy (pagnozzi@portocontericerche.it)

Summary

The available cystic echinococcosis immunodiagnostic tools do not allow cyst viability assessment. Here, synthetic AgB subunits were structurally and immunologically characterized. They all showed propensity to self-oligomerize, similarly to native AgB, and AgB1 held promise as marker of viability.

Running title: AgB synthetic subunits characterization

Abstract

Background: Several tools have been proposed for serodiagnosis of cystic echinococcosis (CE), but none appears promising for cyst viability assessment. Antigens with stage-specific diagnostic value have been described, but few studies with well-characterized antigens and human sera have been performed. Antigen B (AgB) proteoforms hold promise as markers of viability, due to their differential stage-related expression and immunoreactivity.

Methods: Four AgB subunits (AgB1, AgB2, AgB3, AgB4) were synthesized and structurally characterized. Based on the preliminary evaluation of the subunits by western immunoblotting and ELISA, AgB1 and AgB2 were further tested in two ELISA setups, and extensively validated on 422 human sera.

Results: All subunits showed a high degree of spontaneous oligomerization. Interacting residues within oligomers were identified, showing that both N-Terminal and C-Terminal of each subunit are involved in homo-oligomer contact interfaces. No hetero-oligomer was identified. AgB1 and AgB2 ELISAs revealed different sensitivity relative to cyst stage. Of note, besides high specificity (97.2%), AgB1 revealed a higher sensitivity for active-transitional cysts (100% for CE1, 77.8% for CE2, 81.5% for CE3a, and 86.3% for CE3b) than for inactive cysts (41.7% for CE4 and 11.1% for CE5) and post-surgery patients (44%). Interestingly, 19/20 patients with spontaneously inactive cysts and 6/9 treated with albendazole over 5 years earlier were negative on the AgB1 assay.

Conclusions: The structural characterization of subunits provides insights into the synthetic antigen conformation. The stage-related sensitivity of synthetic AgB1 holds promise as part of a multiantigen setting and deserves further longitudinal evaluation as marker of cyst viability.

Keywords: Cystic echinococcosis; AgB; serodiagnosis; structural and immunological characterization; cyst viability.

Introduction

Cystic echinococcosis (CE) is a neglected zoonotic disease caused by the larval stage of the parasite *Echinococcus granulosus* sensu lato, and represents a worldwide public health and economic issue. The parasite life cycle typically includes sheep, goats, swine and cattle among others as intermediate hosts, and canids as definitive hosts, and it is particularly widespread in livestock breeding areas [1]. Humans may act as accidental intermediate hosts by ingestion of parasite eggs in contaminated material. After infection, patients develop fluid-filled cysts that can localize in different organs, mostly liver and lungs, and may remain asymptomatic for years.

Although imaging, especially ultrasound (US) for abdominal localization, is the most reliable tool for diagnosis of CE, serology is a useful complementary tool. However, the performances of current serology tests are unsatisfactory [2, 3].

The World Health Organization Informal Working Group on Echinococcosis (WHO-IWGE) international classification of US images classifies CE cysts in 6 stages [4, 5], which largely reflect the biological viability of cysts: CE1, CE2, CE3b (CE1-2 active cysts, CE3b transitional cyst; all biologically viable), CE3a (transitional cyst; variable viability), and CE4 and CE5 (inactive cysts; biologically non-viable) [6]. However, the biological non-viability of inactive cysts cannot be predicted by US appearance. In particular, CE4 cysts (inactive cysts with solid appearance on US) are in the vast majority of cases non-viable when this stage is reached spontaneously [7-9], while a variable proportion of cases reactivate if CE4 has been reached after medical treatment of an active stage, indicating biological viability [10, 11]. Hence the need for years-long follow-up with US of patients to detect cyst reactivation after treatment, as currently available serology tests are not useful for this purpose [12].

Many investigations evaluated the diagnostic performances of synthetic, native or recombinant purified antigens of *E. granulosus*. Antigen 5 (Ag5) and Antigen B (AgB) are by far the most exploited, due to their abundance and immunogenic properties [13, 14]. AgB is an oligomeric thermostable lipoprotein encoded by 5 genes (AgB1-AgB5), composed of multimers of 8 kDa subunits, [15] mainly secreted by the germinal layer [16], and carrying a large amount of lipids of host origin, which account for almost 50% of its mass. Several studies have investigated the reactivity of AgB1 and AgB2, the most abundant subunits in the native complex [17]. AgB has also been structurally investigated [18-22], revealing an α-helix-rich configuration, with high propensity to oligomerize both in the native and recombinant forms.

Given their abundance and immunogenicity, both Ag5 and AgB have been often proposed as targets in serological assays. However, mixed results have been obtained for these antigens in terms of sensitivity and specificity [13, 14], probably due to the use of different experimental conditions, different panels of sera, limited number of samples, poor inter-laboratory reproducibility of antigen preparations, and lack of antigen characterization, whose structure and immunoreactivity may be very different *in vitro* [2, 23, 24].

To this aim, we have previously highlighted the critical role of a high-quality purification of native Ag5 for developing highly specific serological assays [25, 26]. Different protein targets, including Ag5 and high quality products of the AgB gene variants, might be combined in a multiantigen test for enabling a more reliable serological diagnosis and providing useful indications on cyst viability. However, a rapid, high quality and high yielding purification of native AgB variants represents an unmet challenge, and synthetic products would serve as an excellent alternative. Yet, the structural features of a given synthetic peptide deserve to be investigated to deepen the knowledge on the

possible relationship between the *in vitro* obtained structures and their immunoreactivity in novel serological assays.

Therefore, in this study we characterized the structural features and evaluated the immunoreactivity of four synthetic proteins, corresponding to the subunits AgB1-AgB4, the main constituents of the native AgB complex [18]. We provide evidence of their propensity for oligomerization and report detailed information on interacting residues, as well as the first putative description of AgB homo-oligomers arrangement. Building on these well characterized synthetic antigens, we also extended the evaluation of the different immunoreactivities exhibited by AgB proteoforms carried out by Ahn and coworkers, to cyst stages [17]. To this end, sera from a cohort of patients and healthy controls were tested against synthetic AgB1 and AgB2 in two ELISA setups. The same sera were also assayed with the Ag5 setup [26]. We observed different sensitivities depending on the AgB subunit and cyst stage, and a good association between AgB1 negative ELISA results and the presence of untreated (i.e. spontaneously inactivated) inactive cysts. The comparison of AgB and Ag5 ELISA results opens interesting perspectives on the applicability of a multiantigen test for the assessment of cyst viability and follow-up of patients.

Methods

A detailed description of methods is provided in supplementary file S1.

Synthesis and purification of AgB subunits

AgB1 (7.6 kDa), AgB2 (8.2 kDa), AgB3 (7.7 kDa) and AgB4 (8.2 kDa) sequences were selected from UniProt/KB. Proteins were synthesized, purified and verified by mass spectrometry (MS) [27, 28].

Size exclusion chromatography

Size exclusion chromatography (SEC) was performed on an AKTA Explorer 10 system, and elution profiles were recorded based on the UV absorption at 220 and 280 nm.

Chemical cross-linking experiments

Each AgB subunit or their equimolar mixture were treated with a 100-fold molar excess of 1-ethyl-3-(3-dimethylamino propyl)-carbodiimide (EDC) cross-linking reagent; reactions were stopped, and samples were separated by SDS-PAGE. Selected protein bands were *in situ* digested [30], and analyzed by LC-MS/MS on a Q Exactive mass spectrometer interfaced with an UltiMate 3000 RSLCnano LC system.

Cross-linked peptides were identified using StavroX software (version 3.3.0.1) [32].

Western immunoblotting

Western immunoblotting was performed as described previously [25]. Membranes were incubated with 1:200 Working Standard Anti-Echinococcus Serum, Human (WSH serum).

Samples

A total of 422 blood sera were collected, including 148 from patients with CE cysts, 25 from patients that had previously been treated surgically for CE and in follow-up at the time of serum collection (post-surgery), and 249 from healthy subjects. Table 1 summarizes the number of patients available for each group and the corresponding cyst location.

ELISA

ELISA was performed as described previously [26]. Sera were added at 1:200 dilutions to microplates coated with 100 µL/well of antigen solutions in PBS. To compare results obtained from different plates, a Sample Ratio (SR) was calculated.

Statistical analysis

Data analysis was performed with MedCalc Statistical Software version 15.2.2. ROC curves, McNemar test, and Kruskal-Wallis test were applied to data sets, as previously reported [26].

Results

Structural characterization of AgB subunits

The oligomeric state of AgB1-AgB4 synthetic subunits was investigated by SEC and cross-linking experiments. SEC was performed on the four subunits to study their quaternary structure in phosphate buffer (Figure 1). AgB1 chromatogram resulted in one main peak with an elution volume corresponding to a molecular weight of about 66 kDa, in agreement with an octamer/nonamer (8.8 units) and a very small peak at the dimer's elution volume (17 kDa). For AgB2 and AgB3 one single peak was observed (about 56 and 51 kDa, respectively), both corresponding to esameric/eptameric structures (6.8 and 6.6 units, respectively). AgB4 exhibited only a very small peak, probably due to solubilization issues or high propensity to aggregate, at an apparent molecular weight of about 51 kDa (esamer).

Cross-linking experiments with EDC were performed to covalently stabilize the quaternary structure reached by each subunit or their equimolar mixture, to allow their self-assembling in heteromeric complexes. Products were separated on SDS-PAGE in reducing and non-reducing

conditions (Figures 2A-2B for single subunits and Supplementary Figures S1A-S1B for the mixture, respectively). AgB1 oligomers clearly showed the formation of covalent bonds among subunits upon the addition of EDC, leading to the appearance of bands putatively corresponding to dimers, trimers and tetramers (Figure 2A and 2B, lane 2). Though for AgB2, AgB3, AgB4, and the mixture the effect of cross-linking was less evident, also the gel bands putatively containing their dimers, trimers, tetramers, and, in addition for the mixture, high molecular weight (HMW) species, were excised and analyzed by MS; the monomeric bands were analyzed as a control, to deplete signals deriving from internal cross-links.

After careful attribution of all the interacting residues also found in the monomeric bands, StavroX analysis and manual check of the spectra, a series of cross-linked peptides was detected. Results are summarized in figure 3, Supplementary figure S2 and Supplementary file S2; the MS/MS spectrum of a cross-linked peptide is shown, as an example, in Supplementary Figure S3.

All the evaluated combinations provided information about cross-linked residues, revealing interactions involving both N- and C-terminal regions. The distribution of interacting residues was quite similar among the different subunits, both when they underwent cross-linking by themselves and in the mixture. No hetero-oligomer was identified, suggesting that, at least in our experimental conditions, subunits rearrange, also in an equimolar mixture, as homo-oligomers.

Immunoreactivity of AgB subunits and oligomers

Immunoreactivities of AgB1, AgB2, AgB3, and AgB4 subunits, their combinations and the corresponding cross-linked products were evaluated by western immunoblotting with WSH serum. Results are shown in figure 4. Antigens were tested either as single AgB subunits or as an equimolar mixture. AgB1 showed the highest reactivity, followed by AgB4, AgB2, and AgB3, and the same trend was observed when the subunits were mixed. Non-covalent dimers (Figure 4A) were visible in the absence of EDC, highlighting the stability of their quaternary structure also in

denaturing conditions. A 10-fold excess of cross-linker influenced AgB1, for which a trimer was slightly evident (Figure 4B). A 100-fold excess of EDC, while not showing AgB2, AgB3, and AgB4 reactive oligomers, resulted in the appearance of the AgB1 tetramer and pentamer, producing the classical ladder-like pattern of native AgB (Figure 4C and Supplementary figure S4).

To assess the immunoreactivity of single AgB subunits and of different equimolar assortments also in non denaturing conditions, 25 ng/well, 33 ng/well, 50 ng/well, and 100 ng/well of each protein solution were tested by ELISA, with the WSH serum. The absorbance values revealed different immunoreactivities of the four subunits, according to the following trend: AgB1>AgB2>AgB4>AgB3 (Figure 5). No increase was observed when AgB1 was mixed to any other subunit, compared to the same amount (100 ng) of AgB1 individually coated, whilst the other combinations provided higher or lower absorbance values, depending on the antigens combined.

Validation of AgB1 and AgB2 ELISA setups with a large collection of sera

AgB1 and AgB2 at 25 ng/well were selected for individual validation experiments on a large panel of human sera. To characterize and validate their immunoreactivity, 422 sera from individuals harboring CE cysts in different stages were analyzed by ELISA. The optimal cut-off values were calculated by ROC curves (Figure 6 and Table 2). The areas under the ROC curve (AUC) were 0.959 and 0.923 for AgB1 and AgB2, respectively. At the best SR cut-off value (0.103 and 0.058 for AgB1 and AgB2, respectively), AgB1 and AgB2 ELISAs showed very similar sensitivity towards patients with cysts in active-transitional stages (85.1 *vs* 84.0%, $p = 1.000$) and patients after surgery (44.0% *vs* 56.0%, $p= 0.250$) whilst differences were observed in patients harboring CE4 and CE5 cysts, and healthy controls. The positive rate of patients with CE4 and CE5 cysts was 41.7% and 11.1% for AgB1 ELISA, 69.4% and 38.9% for AgB2 ELISA. Specificity of AgB1 was higher than that of AgB2 (97.2% *vs* 83.9%) as tested on sera from healthy controls. Results are summarized in table 3. Both ELISAs discriminated patients and healthy controls (Figures 7A and

7B). Statistically significant differences were also found between patients with active-transitional *versus* the inactive CE cysts (Figures 7C and 7D). Results obtained with sera according to cyst stages are shown in figure 7E and 7F. AgB2 ELISA behaved differently from AgB1, as only CE5 patients and healthy donors showed significant differences from other subgroups.

Finally, AgB1 ELISA results were compared with the ones obtained with Ag5 [26], using the same 422 sera (Table 4). AgB1 specificity was higher than Ag5, although this difference was not statistically significant. Further, AgB1 was significantly less sensitive than Ag5 in detecting patients with cysts in any stage, but especially with inactive cysts. Noteworthy, when patients with inactive cysts were further grouped into i) patients with spontaneously inactivated (untreated) cysts, and treated with albendazole either ii) less or iii) more than 5 years previously (and thus inactivated as the result of treatment), 10/20 untreated patients with inactive cysts, 23/25 and 8/9 treated with albendazole less or more than 5 years earlier, respectively, were positive to Ag5 (Figure 8A), and only 1/20, 13/25 and 3/9, to AgB1 (Figure 8B). Moreover, when the same grouping was evaluated for patients with active-transitional cysts, Ag5 tested positive to 22/25 untreated patients and to 68/69 patients who ended albendazole intake less than 5 years before the collection of serum, whilst AgB1 results were positive for 21/25 and 58/69, respectively.

Discussion

The search for a marker of cyst viability, to complement US staging, is one of the challenges in the field of clinical CE. The results of serodiagnostic tests are still unreliable from a clinical point of view. Several studies have been performed on small/medium/large panels of human sera, mostly involving a limited number of immunodominant proteins [13, 14]. The most extensively investigated and promising antigens are Ag5 and AgB, due to their strong immunoreactivity and relatively high abundance in hydatid fluid. Both have been tested as native, recombinant and synthetic antigens [13, 14], with conflicting results. A number of features make AgB a good

candidate biomarker of CE development and progression. Among others, its primary secretion by the germinal layer cells [16], its putative involvement in the parasite lipid metabolism and as potential ligand for monocyte and macrophage receptors [22, 37], the variation of its relative abundance, specific oligomer assortments, and/or exposition to the immune system at different CE stages [17]. From a structural point of view, some information on this antigen was provided by other authors, both on recombinant subunits, and on native AgB complex [18, 19, 38]. Understanding the protein conformation can help to explain its immunoreactivity, and provide information about the host-parasite interplay. Nevertheless, we are not aware of previous studies combining structural and immunological studies of this CE antigen. Here, a detailed structural and immunodiagnostic investigation of the synthetic proteins constituting the four main subunits of the native AgB complex was carried out. According to the conformational studies, the ability of all the synthetic proteins to form oligomeric structures was shown for the first time. Our results suggest that the four subunits rearrange into highly organized structures, up to nonamers, and that interactions involve both the N- and the C-terminal regions, as the subunits would be organized in parallel and/or antiparallel bundles, maybe generating channels where lipids can be accommodated. As already suggested [18], we hypothesize that *in vivo* each subunit may act as a nucleation center whose propagation leads to high order oligomers, also building on the presence of other compounds or external stimuli. Among the subunits, the most cross-linked was AgB3, confirming the previous observation about a more compact structure that could also be responsible for a lower immunoreactivity [18]. Further, the proposed mechanism might explain the lack of conformational data obtained by both structural approaches on AgB4, whose low solubility may be due to its high propensity to oligomerize up to aggregation.

Though showing a similarity with AgB3 in the distribution of contact residues, AgB1 and AgB2 results indicated a higher flexibility, maybe responsible for their higher immunoreactivity. Further studies are warrant to confirm these hypotheses and elucidate their relevance, if any, in host-parasite

interplay. Moreover, our experimental conditions were not able to stabilize any hetero-oligomer, but other experiments exploring different setups and also different approaches, would be required. Finally, AgB homo-oligomers partially survive SDS-PAGE (Figures 2 and 4), although to a lower extent than native AgB. Our results agree with the previous observation that self-assembly does not depend on the presence of lipids, but in their absence oligomers may be smaller than in native complex [38].

Having demonstrated the ability of synthetic subunits to mimic the native antigen, their immunoreactivity was tested. Serological assays based on synthetic subunits showed a clear immunoreactivity with sera from patients with CE both in western immunoblotting and ELISA, with differences between assays mostly involving AgB4. The AgB4 behavior might be explained again by the different assay conditions, and the low solubility of AgB4 in phosphate buffer.

Both AgB1 and AgB2, the most reactive antigens, demonstrated a good sensitivity towards active-transitional stages. On the contrary, especially AgB1 was poorly sensitive in patients with inactive cysts and post-surgery. When we investigated further this noteworthy result, we found that AgB1 was very poorly sensitive towards patients with spontaneously inactive cysts (who had never received albendazole therapy) and patients with inactive cysts resulting from the treatment of active cysts (who had finished their last course of albendazole more than 5 years previously and for which it is plausible to suppose biological non-viability). This finding suggests that AgB1 could be of use to discriminate between inactive cysts that are no longer biologically viable and those still biologically viable and therefore requiring a longer/closer follow-up with US to detect reactivation. However, these results need confirmation with a longitudinal study evaluating responses to AgB along the evolution of CE4 cysts over time. Also, our data strongly support the use of both Ag5 and AgB1 in a multiantigen configuration, to provide both high sensitivity for diagnosis of CE, and information on cyst viability, to guide the follow-up approach.

Antigen combinations should be further explored to identify the optimal setup conditions for developing a highly performing diagnostic test.

Notes

Acknowledgments

The authors thank the “HERACLES” extended network (http://www.Heracles-fp7.eu/), for the useful discussions among the members.**Financial support**

This work was supported by Regione Autonoma della Sardegna [art. 9 LR 20/2015].

Potential conflicts of interest

The authors declare no conflict of interest. All authors have submitted the ICMJE Form for Disclosure of Potential Conflicts of Interest.

References

1. Deplazes P, Rinaldi L, Alvarez Rojas CA, et al. Global Distribution of Alveolar and Cystic Echinococcosis. Adv Parasitol, **2017**; 95:315-493.
2. Hernández-González A, Santivañez S, García HH, et al. Improved serodiagnosis of cystic echinococcosis using the new recombinant 2B2t antigen. PLoS Negl Trop Dis, **2012**; 6:e1714.
3. Lissandrin R, Tamarozzi F, Piccoli L, et al. Factors Influencing the Serological Response in Hepatic Echinococcus granulosus Infection. Am J Trop Med Hyg, **2016**; 94:166-71.
4. WHO Informal Working Group. International classification of ultrasound images in cystic echinococcosis for application in clinical and field epidemiological settings. Acta Trop, **2003**; 85: 253–261.
5. Brunetti E, Kern P, Vuitton DA; Writing Panel for the WHO-IWGE. Expert consensus for the diagnosis and treatment of cystic and alveolar echinococcosis in humans. Acta Trop, **2010**; 114:1-16.
6. Hosch W, Junghanss T, Stojkovic M, et al. Metabolic viability assessment of cystic echinococcosis using high-field 1H MRS of cyst contents. NMR Biomed, **2008**; 21:734-54.
7. Piccoli L, Tamarozzi F, Cattaneo F, et al. Long-term sonographic and serological follow-up of inactive echinococcal cysts of the liver: hints for a "watch-and-wait" approach. PLoS Negl Trop Dis, **2014**; 8:e3057.
8. Stojkovic M, Rosenberger KD, Steudle F, Junghanss T. Watch and Wait Management of Inactive Cystic Echinococcosis- Does the Path to Inactivity Matter - Analysis of a Prospective Patient Cohort. PLoS Negl Trop Dis, 2016; 10:e0005243.
9. Solomon N, Kachani M, Zeyhle E, Macpherson CNL. The natural history of cystic echinococcosis in untreated and albendazole-treated patients. Acta Trop, 2017; 171:52-57.

10. Stojkovic M, Zwahlen M, Teggi A, et al. Treatment response of cystic echinococcosis to benzimidazoles: a systematic review. PLoS Negl Trop Dis, **2009**; 3:e524.
11. Rinaldi F, De Silvestri A, Tamarozzi F, Cattaneo F, Lissandrin R, Brunetti E. Medical treatment versus "Watch and Wait" in the clinical management of CE3b echinococcal cysts of the liver. BMC Infect Dis, **2014**; 14:492.
12. Hernández-González A, Muro A, Barrera I, Ramos G, Orduña A, Siles-Lucas M. Usefulness of four different Echinococcus granulosus recombinant antigens for serodiagnosis of unilocular hydatid disease (UHD) and postsurgical follow-up of patients treated for UHD. Clin Vaccine Immunol, **2008**; 15:147-53.
13. Manzano-Román R, Sánchez-Ovejero C, Hernández-González A, Casulli A, Siles-Lucas M. Serological Diagnosis and Follow-Up of Human Cystic Echinococcosis: A New Hope for the Future? Biomed Res Int, **2015**; 2015:428205.
14. Díaz A, Casaravilla C, Barrios AA, Ferreira AM. Parasite molecules and host responses in cystic echinococcosis. Parasite Immunol, **2016**; 38:193-205.
15. Obal G, Ramos AL, Silva V, et al. Characterisation of the native lipid moiety of Echinococcus granulosus antigen B. PLoS Negl Trop Dis, **2012**; 6:e1642.
16. Virginio VG, Monteiro KM, Drumond F, et al. Excretory/secretory products from in vitro-cultured Echinococcus granulosus protoscoleces. Mol Biochem Parasitol, **2012**; 183:15-22.
17. Ahn CS, Han X, Bae YA, et al. Alteration of immunoproteome profile of Echinococcus granulosus hydatid fluid with progression of cystic echinococcosis. Parasit Vectors, **2015**; 8:10.
18. Monteiro KM, Cardoso MB, Follmer C, et al. Echinococcus granulosus antigen B structure: subunit composition and oligomeric states. PLoS Negl Trop Dis, **2012**; 6:e1551.

19. Monteiro KM, Scapin SM, Navarro MV, et al. Self-assembly and structural characterization of Echinococcus granulosus antigen B recombinant subunit oligomers. Biochim Biophys Acta, **2007**;1774:278-85.
20. Monteiro KM, Zaha A, Ferreira HB. Recombinant subunits as tools for the structural and functional characterization of Echinococcus granulosus antigen B. Exp Parasitol, 2008; 119:490-8.
21. González G, Nieto A, Fernández C, Orn A, Wernstedt C, Hellman U. Two different 8 kDa monomers are involved in the oligomeric organization of the native Echinococcus granulosus antigen B. Parasite Immunol, **1996**; 18:587-96.
22. Silva-Álvarez V, Folle AM, Ramos AL, et al. Echinococcus granulosus antigen B: a Hydrophobic Ligand Binding Protein at the host-parasite interface. Prostaglandins Leukot Essent Fatty Acids, **2015**; 93:17-23.
23. Ito A Nothing is perfect! Trouble-shooting in immunological and molecular studies of cestode infections. Parasitology, **2013**; 140:1551-65.
24. Tawfeek GM, Elwakil HS, El-Hoseiny L, et al. Comparative analysis of the diagnostic performance of crude sheep hydatid cyst fluid, purified antigen B and its subunit (12 Kda), assessed by ELISA, in the diagnosis of human cystic echinococcosis. Parasitol Res, **2011**; 108:371-6.
25. Pagnozzi D, Biosa G, Addis MF, Mastrandrea S, Masala G, Uzzau S. An easy and efficient method for native and immunoreactive Echinococcus granulosus antigen 5 enrichment from hydatid cyst fluid. PLoS One, **2014**; 9:e104962.
26. Pagnozzi D, Addis MF, Biosa G, et al. Diagnostic Accuracy of Antigen 5-Based ELISAs for Human Cystic Echinococcosis. PLoS Negl Trop Dis, **2016**; 10:e0004585.
27. Addis MF, Tedde V, Dore S, et al. Evaluation of milk cathelicidin for detection of dairy sheep mastitis. J Dairy Sci, **2016**; 99:6446–56.

28. Mura S, Greppi G, Roggio AM, Malfatti L, Innocenzi P. Polypeptide binding to mesostructured titania films. Microp Mesop Mater, **2011**; 142:1-8.
29. Laemmli UK. Cleavage of structural proteins during the assembly of the head of bacteriophage T4. Nature, **1970**; 227:680–5.
30. Tanca A, Pagnozzi D, Burrai GP, et al. Comparability of differential proteomics data generated from paired archival fresh-frozen and formalin-fixed samples by GeLC-MS/MS and spectral counting. J Proteomics, **2012**; 77:561-76.
31. Schlosser A, Volkmer-Engert R. Volatile polydimethylcyclosiloxanes in the ambient laboratory air identified as source of extreme background signals in nanoelectrospray mass spectrometry. J Mass Spectrom, **2003**;38:523-5.
32. Götze M, Pettelkau J, Schaks S, et al. StavroX—A Software for Analyzing Crosslinked. J Am Soc Mass Spectrom, **2012**; 23:76-87.
33. DeLong ER, DeLong DM, Clarke-Pearson DL Comparing the areas under two or more correlated receiver operating characteristic curves: a nonparametric approach. Biometrics, **1988**; 44:837-45.
34. Bantis LE, Nakas CT, Reiser B. Construction of confidence regions in the ROC space after the estimation of the optimal Youden index-based cut-off point. Biometrics, **2014**; 70:212-23.
35. Conover WJ. Practical Nonparametric Statistics. 3rd edition, Hoboken: Wiley, **1999**.
36. Burra P, Arcidiacono D, Bizzaro D, et al. Systemic administration of a novel human umbilical cord mesenchymal stem cells population accelerates the resolution of acute liver injury. BMC Gastroenterol, **2012**; 12:88.
37. Silva-Álvarez V, Folle AM, Ramos AL, et al. Echinococcus granulosus Antigen B binds to monocytes and macrophages modulating cell response to inflammation. Parasites & Vectors, **2016**; 9:69.

38. Silva-Álvarez V, Franchini GR, Pórfido JL, Kennedy MW, Ferreira AM, Córsico B. Lipid-free antigen B subunits from echinococcus granulosus: oligomerization, ligand binding, and membrane interaction properties. PLoS Negl Trop Dis, **2015**; 9:e0003552.

Figure legends

Figure 1. Size exclusion chromatography of the synthetic AgB subunits. The chromatogram overlay of AgB1 (solid line), AgB2 (dashed line), AgB3 (dash dotted line) and AgB4 (dotted line) shows their similar propensity to oligomerize. $(AgBm)_n$ indicates the n units forming the AgBm oligomer. Size calibration marks, obtained from runs of standard proteins Aprotinin, 6.5 kDa, Ribonuclease A, 13.7 kDa, Carbonic Anhydrase, 29 kDa, Ovalbumin, 44 kDa, Conalbumin, 75 kDa and Blue Dextran 2000, as void volume V_0, are indicated by arrows in the chromatogram.

Figure 2. SDS-PAGE of synthetic AgB subunits and their cross-linking products under reducing (panel a) and non-reducing conditions (panel b). Lanes 1, 3, 5 and 7 correspond to the individual subunits without the addition of EDC reagent. Lanes 2, 4, 6 and 8 correspond to the individual subunits after incubation with EDC reagent.

Figure 3. Interacting residues from MS analysis of protein bands after incubation of single subunits with EDC.

Figure 4. Western immublotting of synthetic AgB subunits (panel a) and their cross-linking products after incubation with a 10-fold (panel b), or a 100-fold (panel c) excess of EDC under reducing conditions, as individual components, or as a mixture of the four subunits.

Figure 5. ELISA absorbance values using the synthetic subunits as antigens. Different amounts of each synthetic subunit (25, 33, 50 and 100 ng) and their equimolar combination (100 ng of total mixture) evaluated against the WSH serum. A dashed line indicates the absorbance value obtained in the same conditions, on an uncoated well. Bars indicate the standard deviation from the mean.

Figure 6. ROC curves overlay of the AgB1 (solid line) and AgB2 (dashed line) ELISA setups. Curves are generated by plotting Sensitivity *versus* 100-Specificity.

Figure 7. Box-and-whiskers plots of ELISA results for AgB1 and AgB2 setups, (left and right panels, respectively). Boxes indicate values falling within the 25^{th} and 75^{th} percentiles (InterQuartile Range, IQR). Central lines represent the median values. Whiskers indicate values falling within the ±1.5*IQR. Single dots depict values falling outside the whiskers. Dashed lines indicate the best cut-off values. **= statistically different groups after Kruskal-Wallis test, or after Conover test, with Bonferroni correction, for multiple comparisons. According to this adjustment, to achieve statistical significance three different *p*-value have been considered: $p < 0.05$ for panels a, and b; $p < 0.017$ for panels c and d; $p < 0.0018$ for panels e, and f. Groups significantly different in panels e, and f are indicated as (* group). PS: post-surgery; H: healthy donors.

Figure 8. Box-and-whiskers plots of ELISA results for Ag5 and AgB1 setups, (left and right panels, respectively). Boxes indicate values falling within the 25^{th} and 75^{th} percentiles (InterQuartile Range, IQR). Central lines represent the median values. Whiskers indicate values falling within the ±1.5*IQR. Single dots depict values falling outside the whiskers. Dashed lines indicate the best cut-off values. Statistically different groups after Kruskal-Wallis test, coupled to Conover test, with Bonferroni correction, for multiple comparisons ($p < 0.017$), are indicated as **.

Tables

Table 1. Patient grouping according to clinical characteristics and location of the cysts with the stage likely most influencing their serological status.

Group	Number of patients	No ABZ treatment	ABZ <5 years	ABZ >5 years	Hepatic cysts	Extra hepatic cysts
CE1	7	2	5	0	7 (100.0%)	0
CE2	9	2	7	0	9 (100%)	0
CE3a	27	7	20	0	26 (96.3%)	1 (3.7%)
CE3b	51	14	37	0	44 (86.3%)	7 (13.7%)
CE4	36	8	23	5	34 (94.4%)	2 (5.6%)
CE5	18	12	2	4	16 (88.9%)	2 (11.1%)
Post-surgery	25	0	25	0	21 (84.0%)	4 (16.0%)
Total	173	45	119	9	157 (90.8%)	16 (9.2%)

ABZ: albendazole.

ABZ <5 years: patients who ended ABZ intake less than 5 years before the collection of serum used for this study.

ABZ >5 years: patients who ended ABZ intake more than 5 years before the collection of serum used for this study.

Table 2. Statistical parameters of the AgB1 ELISA and AgB2 ELISA at the best cut-off values.

Antigen	% Sensitivity	% Specificity	AUC(±SE)	AUC CI (95%)	Youden index	(+LR)	(-LR)
AgB1	85.11	97.19	0.959 (±0.012)	0.932-0.977	0.8230	30.27	0.15
AgB2	84.04	83.94	0.923(±0.015)	0.889-0.949	0.6798	5.23	0.19

AUC: Area Under the Curve. SE: Standard Error. CI: Confidence Interval. +LR: Positive Likelihood Ratio. –LR: Negative Likelihood Ratio.

Table 3. ELISA results by group.

Group		N. of patients	Positive by AgB1	Positive by AgB2	*p* – values
Active-Transitional	**Total**	**94**	**80 (85.1%)**	**79 (84.0%)**	**1.0000**
	CE1	7	7 (100.0%)	5 (71.4%)	0.5000
	CE2	9	7 (77.8%)	8 (88.9%)	1.0000
	CE3a	27	22 (81.5%)	25 (92.6%)	0.3750
	CE3b	51	44 (86.3%)	41 (80.4%)	0.5811
Inactive	**Total**	**54**	**17 (31.5%)**	**32 (59.3%)**	**0.0007***
	CE4	36	15 (41.7%)	25 (69.4%)	0.0129*
	CE5	18	2 (11.1%)	7 (38.9%)	0.0625
Post-surgery	**Total**	**25**	**11 (44.0%)**	**14 (56.0%)**	**0.2500**
Healthy controls	**Total**	**249**	**7 (2.8%)**	**40 (16.1%)**	**< 0.0001***

* Statistically significant difference (McNemar test).

Table 4 Ag5 ELISA serological results and comparison with AgB1 ELISA.

Group		N. of patients	Positive by Ag5	*p* - values
	Total	**94**	**90 (95.7%)**	**0.0309***
	CE1	7	7 (100.0%)	n.a.
Active-Transitional	CE2	9	9 (100%)	0.5000
	CE3a	27	26 (96.3%)	0.2188
	CE3b	51	48 (94.1%)	0.3438
	Total	**54**	**41 (75.9%)**	**< 0.0001***
Inactive	CE4	36	31 (86.1%)	0.0001*
	CE5	18	10 (55.6%)	0.0078*
Post-surgery	**Total**	**25**	**19 (76.0%)**	**0.0078***
Healthy controls	**Total**	**249**	**13 (5.2%)**	**0.2101**

* Statistically significant difference (McNemar test). n.a.= not applicable.

Figure 1

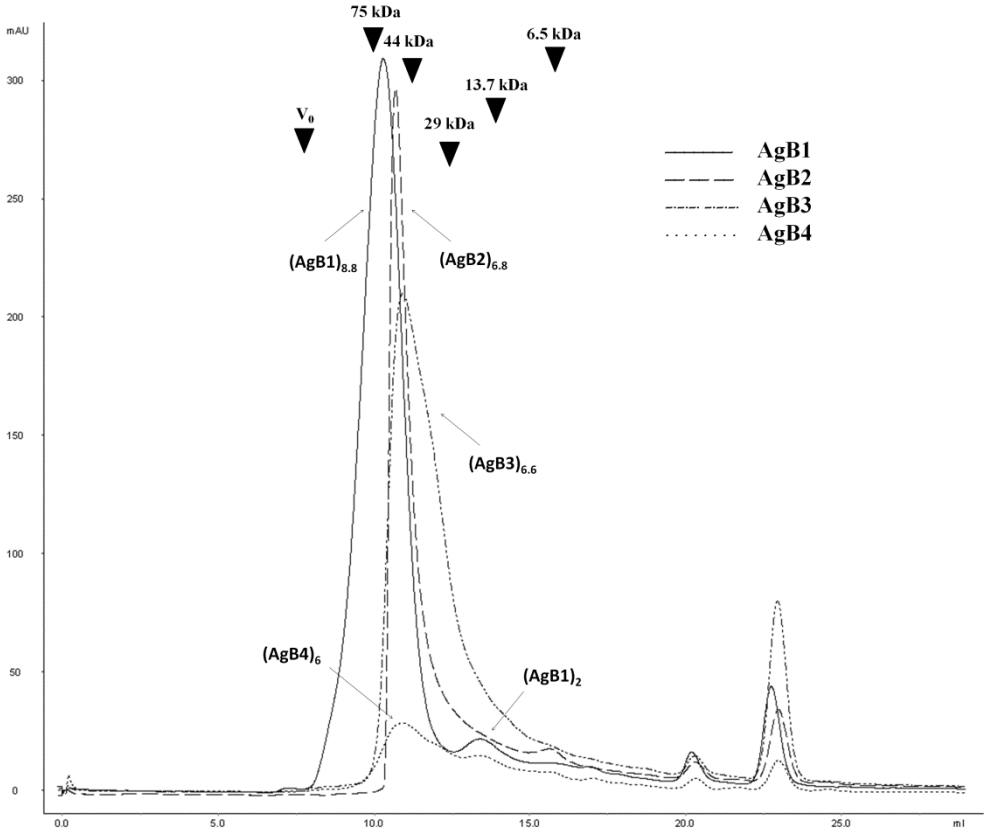

Figure 2

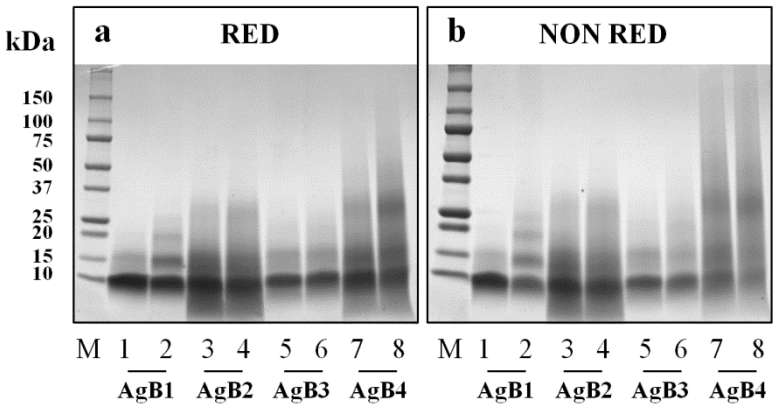

Figure 3

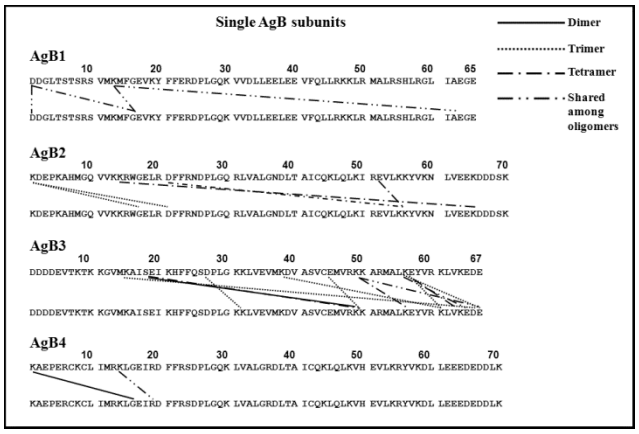

Figure 4

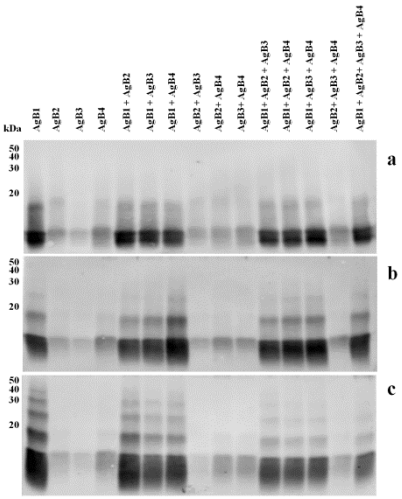

Figure 5

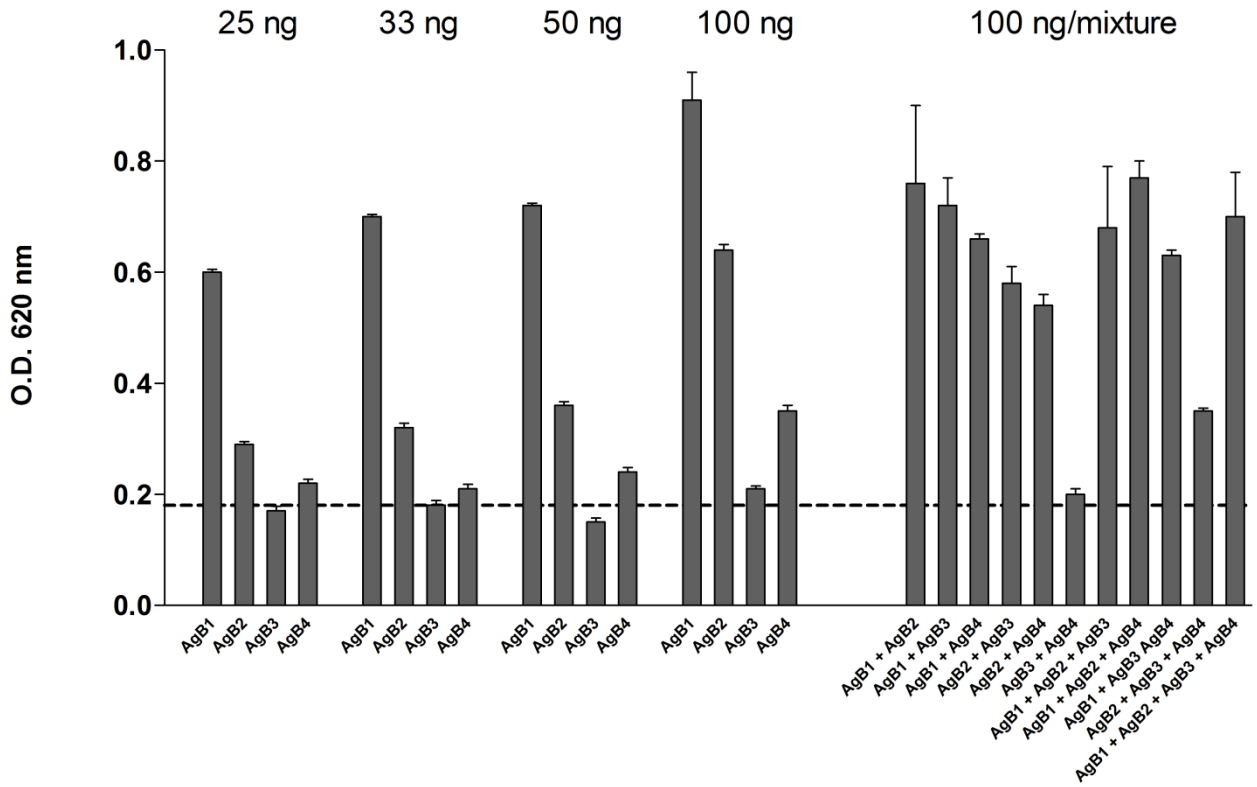

Figure 6

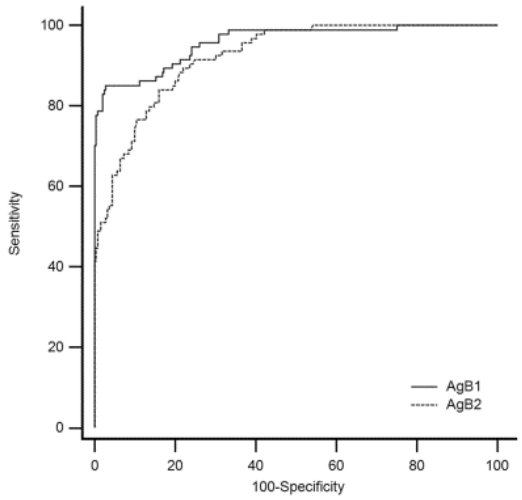

Figure 7

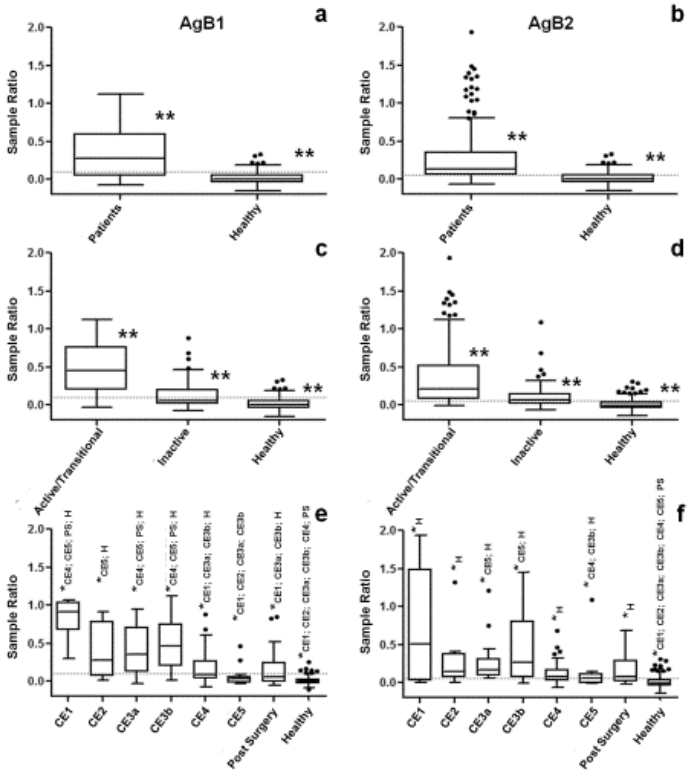

Figure 8